

Chemical Potential Maps and Spatial Correlations in 2D-Island Ripening on Si(001)

W. Theis,¹ N. C. Bartelt,² and R. M. Tromp¹

¹IBM Research Division, T. J. Watson Research Center, P. O. Box 218, Yorktown Heights, New York 10598

²Department of Physics, University of Maryland, College Park, Maryland 20742

(Received 10 April 1995)

We have used low energy electron microscopy to study the roles of surface diffusion and step-edge attachment kinetics in 2D-island ripening, a phenomenon closely related to epitaxial growth. From experimental maps of the chemical potential, showing variations of up to a factor of 3, we conclude that nearest-neighbor correlations between islands are of central importance, in contrast to common mean-field theory. Detailed simulations of the time evolution of specific island configurations are in close agreement with experimental results.

PACS numbers: 68.10.Jy, 61.16.-d, 68.35.Bs, 68.35.Md

Epitaxial growth is one of the central processes used and studied in surface science. A progression of distinct elements is essential for understanding how a characteristic surface morphology evolves from atoms hitting the surface at random locations. Starting with an understanding of equilibrium island shapes and step energetics and dynamics in the absence of an incoming atom flux [1], we now progress to a study of the mechanisms involved in the equilibration of a given configuration of islands on the surface. A detailed understanding of this coarsening process towards fewer and larger islands, called Ostwald ripening [2], driven by the free energy cost of the islands' step edges, can serve as the basis for future studies addressing the nucleation of new islands during growth.

In this Letter we explore the ripening of 2D islands on Si(001), going beyond ensemble averages of earlier experiments on 2D and 3D island ripening [3–6] and following the time evolution of individual islands in relation to the configuration of neighboring islands. We extract a chemical potential map from the experiment showing local variations of as much as a factor of 3, and we introduce a nearest-neighbor model reproducing this large variation. Simulating the time evolution of the island configuration using both mean-field theory and the nearest-neighbor model, we demonstrate the importance of local correlations in accurately describing 2D island ripening on Si(001).

The experiment was performed by depositing about one-tenth of a monolayer of Si on Si(001) at room temperature. After a rapid increase of the temperature to 670 °C at $t = 0$, the subsequent evolution of an initially step free region of 5 μm diameter was imaged by low-energy electron microscopy (LEEM) [7], and recorded on videotape. Figures 1(a) and 1(b) show LEEM images at two different times. They were recorded in dark field imaging mode with a half order diffraction beam corresponding to one of the two orientations of the (2×1) dimer reconstruction. The orientation alternates with every additional atomic layer, thus the bright elliptic

islands [Figs. 1(a) and 1(b)] are one atomic layer higher than the surrounding terrace.

Except for rare cases when islands contain (2×1) domain boundaries due to out of registry coalescence in the initial stages ($t < 50$ s) of the experiment, all islands are ellipses with an aspect ratio of ~ 2.6 [1]. The dimer rows are parallel to the long axis of the islands. There is no appreciable shift with time of the center of mass of the individual islands, except for those near the bounding step. The island coverage on the terrace decreases from 7.4% at 50 s to 5.7% at 400 s.

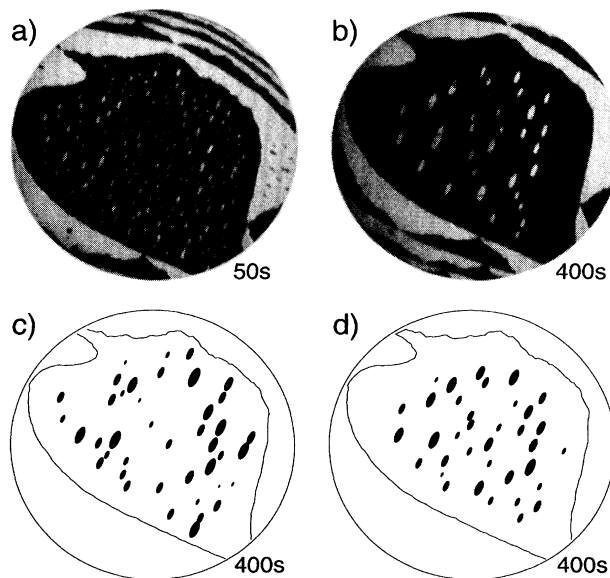


FIG. 1. Experimental and simulated island configurations on Si(001). Panels (a) and (b) show LEEM images at 50 and 400 s after the temperature was raised to 670 °C. Alternate dark and bright regions differ in height by one atomic layer. The field of view is 5.5 μm . The experimental image at 400 s is contrasted with the island configurations resulting from propagating the experimental configuration at 50 and 400 s using a mean-field [panel (c)] and a nearest-neighbor approach [panel (d)].

To analyze the video sequences, the recorded images were digitized at a rate of one per second. The images were converted to black and white by thresholding them at an appropriate grey level. Connected white regions were identified as islands, their position and area given by the center of mass and the number of bright pixels, respectively.

In giving a theoretical description of the ripening process, the nature of the exchange of the diffusive species (believed to be dimers, but forthwith loosely termed adatoms) between the adatom sea and the islands is a key point of interest. The adatom concentration on the terrace obeys a normal diffusion equation, and the Gibbs-Thomson chemical potential of an island with radius R is simply proportional to $1/R$. At one extreme, the equilibrium of the chemical potential at the island edge is much faster than the equilibration of the concentration profile in the adatom sea. This leads to a diffusion limited case in which the chemical potential is continuous across the island's edges and the change of an island's size is determined by the gradient in the surrounding adatom sea. Or, in the case limited by attachment and detachment kinetics at the step edge, the adatom sea equilibrates faster, producing a discontinuity of the chemical potential across island edges. The flux from each island is proportional to the magnitude of the discontinuity of the chemical potentials at the island edge times the island's circumference.

To distinguish between these two cases it is most convenient to study the evolution of a disappearing isolated island on a large terrace. In Fig. 2(a) we show the measured time dependence of the area of such an island (from a different experiment than the one presented in Fig. 1), showing a linear decrease in island area with time. This agrees with the predictions of the attachment or detachment limited case, where the adatom chemical potential becomes negligible compared to the island chemical potential for sufficiently small islands, resulting in a flux proportional to the island's circumference times $1/R$, i.e., the island area decreases linearly with time. The data are clearly inconsistent with the $t^{2/3}$ dependence found for diffusion limited ripening [8]. From temperature dependent studies of the single-island dissolution rate we determine an activation energy of 1.2 eV [9], identical to the activation energy for attachment limited step-edge fluctuations [1]. Thus, we find that ripening and step-edge fluctuations are described in a common framework in which the flux of atoms step edges onto the terraces is limited by attachment or detachment kinetics.

Since the ripening process is governed by the chemical potential difference at the island edges, we characterize the adatom sea by an effective chemical potential μ_{ad} defined at the sites of the islands and forgo taking the diffusion equation into account. The conservation of total

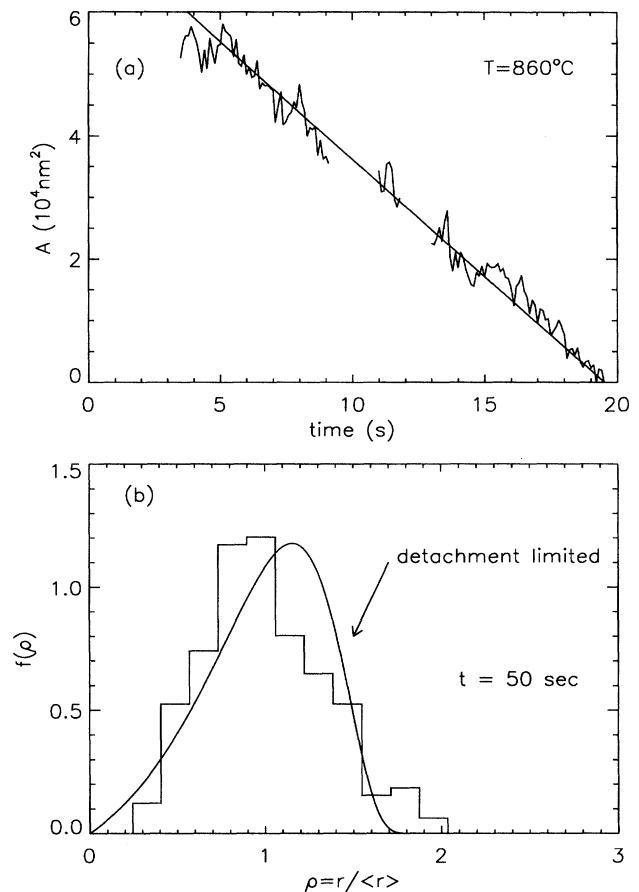


FIG. 2. Panel (a) shows the time dependence of the area of an isolated island on Si(100) at 860 °C. The linear decrease is indicative of ripening limited by attachment or detachment kinetics and not by diffusion. In panel (b), the experimental island size distribution at 50 s is compared with predictions of the attachment or detachment limited mean-field theory of Ostwald ripening.

island area must then be included as an explicit boundary condition.

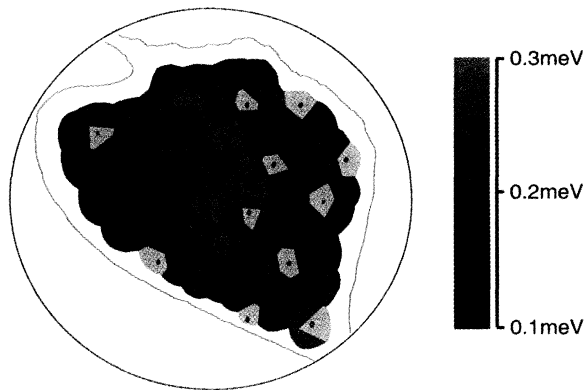
First, we will discuss the classical mean-field theory in which μ_{ad} is taken to be uniform, its value being inversely proportional to the mean island radius in order to attain area conservation. In this framework the late stage island size distribution can be calculated analytically [9,10]. Figure 2(b) shows that the experimental island size distribution at $t = 50$ s is fairly well reproduced by the mean-field predictions for the attachment or detachment limited case. This good agreement is also found at later times, although with the decreasing number of islands the statistics become poorer.

In the past, comparison of the island size distribution with mean-field predictions has been the most common method of evaluating the applicability of mean-field the-

ory. Here we show that, despite the reasonable agreement between experimental and mean-field distributions, mean-field theory is not successful in describing individual islands or local properties. We do this first by showing explicitly that the chemical potential of the adatom sea is not uniform, in contrast with the mean-field assumption.

Having established the validity of the attachment or detachment mechanism in which the island growth rate is proportional to the difference between the island and adatom chemical potential, we can determine the value of the chemical potential at the site of each island by measuring each island's growth rate. Figure 3(a) depicts the resulting chemical potential map of the surface at $t = 100$ s, where the color scale from blues to red correspond to a factor of 3 increase in μ_{ad} , and the absolute values (in meV) are based on step-edge free energies deduced

a) Experiment at 100s



b) Nearest-neighbor theory

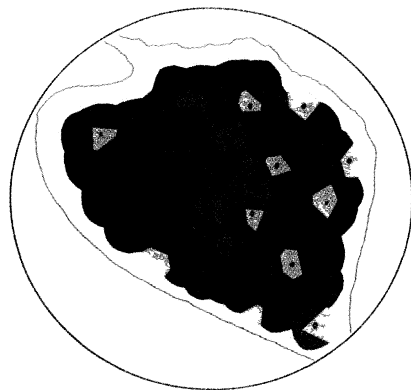


FIG. 3(color). Comparison of the experimentally determined chemical potential map at 100 s [panel (a)] with the results of the nearest-neighbor model [panel (b)]. Gray areas in the experimental plot indicate islands that are too small to derive a reliable chemical potential from. The Voronoi polygon surrounding each island is colored according to the chemical potential obtained from a measurement of the island's growth rate.

in Ref. [1]. In agreement with scaling in ripening, the magnitude of the variation at later times is similar. Areas close to the bounding edge or surrounded by islands predominantly larger than average tend to exhibit a low chemical potential, as one would expect. A model that reproduces these variations in the chemical potential would also succeed in matching the experimental evolution of the individual islands in the ripening process.

To explicitly demonstrate that mean-field theory with its inherently uniform chemical potential cannot successfully describe the evolution of individual islands, we have performed a mean-field simulation. Taking the experimental island configuration at $t = 50$ s [Fig. 1(a)] as the starting configuration, we calculated the mean-field value of the adatom chemical potential and the area change of every island from the rate equation, gaining the new island configuration for a slightly later time. Iterating this procedure gives the time evolution of the island configuration in the simulation. The time scale of the simulation is set by matching the rate by which the average island size increases to the experimental data. The resulting mean-field configuration at 400 s [Fig. 1(c)] differs significantly from the corresponding experimental configuration [Fig. 1(b)]. The mean-field theory shows a rapid depletion of islands in the center and an overabundance at the edges of the terrace, in obvious disagreement with the experimental result [Fig. 1(b)].

Having established the need for a model that features a high degree of nonuniformity in the chemical potential, we turn to the particularly simple case in which the chemical potential at the site of a given island depends only on its nearest-neighbor islands, determined by the Voronoi construction [11]. For each pair of neighboring islands we define the area conserving chemical potential proportional to one over their mean radius, as in the mean-field case. For a given island we have a number of chemical potentials—one for every pairing with a neighboring island. The resulting effective chemical potential for the adatom sea at the site of the island is an appropriately weighted average of these. To assure area conservation, every pairwise chemical potential must contribute equally to the respective pair of sites. Since the number of neighbors varies from island to island, a simple average does not accomplish this. The appropriate weight is given by $1/2\pi$ times the opening angle from the island towards the separating segment in the Voronoi construction corresponding to the particular neighbor. This also has the favorable side effect of making the effective chemical potential insensitive against abrupt changes in the number of neighbors caused by only slight changes in island positions. In this model the total adatom currents can be reduced to local currents between neighboring pairs of islands depending only on the particular pairs of islands and its weight derived from the Voronoi construction.

In Fig. 3(b) we present the map of the effective chemical potential for the nearest-neighbor model at 100 s. The bounding step edge is treated as an island of infinite radius. A comparison with the experimental result [Fig. 3(a)] shows that this theory reproduces the overall magnitude and spatial dependence of the observed variations in chemical potential. To quantify how good this agreement is, we have numerically propagated the experimental configuration at 50 to 400 s, getting a good semblance of the experimental result, vastly improving on the mean-field simulation [Fig. 1(d)]. In the simulation we have used one adjustable parameter to get the proper time scale. It represents the rate at which an island in a zero effective chemical potential disappears. The value of $-144 \text{ nm}^2/\text{s}$ is in good agreement with the rate of $-190 \pm 40 \text{ nm}^2/\text{s}$ measured from the dissolution rate of small islands, as well as with the rate of $-100 \text{ nm}^2/\text{s}$ extrapolated (within a factor of 3 uncertainty) from the study of step-edge fluctuations between 790 and 1100 °C (Refs. [1,9]).

The excellent performance of the nearest-neighbor model shows that there is a high correlation of the adatom chemical potential, and thereby the adatom concentration, on a length scale comparable to the mean distance between nearest-neighbor islands. From an additional set of simulations that take diffusion into account *explicitly*, we find a diffusion coefficient on the order of $30\,000 \text{ nm}^2/\text{s}$ and a very good agreement between this more detailed simulation and the nearest-neighbor model [9]. While the resulting diffusion length for 100 s is larger than the field of view, islands act as sources and drains of atoms, screening the diffusional fields of individual islands on a length scale comparable to the island separation [2,5,9,10]. The diffusion coefficient can independently be estimated from the gradient of the adatom chemical potential near the bounding step edges and the net flux towards those step edges, yielding a value of $\sim 70\,000 \text{ nm}^2/\text{s}$. These estimates of the diffusion coefficient are in good agreement with the value of $\sim 45\,000 \text{ nm}^2/\text{s}$ extrapolated from studies of the time evolution of periodic step arrays by Keeffe, Umbach, and Blakely [12].

We conclude that ripening on Si(001) is governed by both attachment or detachment kinetics and diffusion. An experimentally determined map of the chemical potential shows local variations up to a factor of 3. We presented a nearest-neighbor model which reproduces these variations, as well as the evolution of the individual islands. The instantaneous rate of the change of the area of a

given island is attachment or detachment limited, driven by the difference between the chemical potential of the island and the surrounding adatom sea. But the length scale over which the adatom sea equilibrates is limited by diffusion, giving rise to strong nearest-neighbor island correlations in the ripening process, in sharp contrast to simple mean-field theory. The values obtained for the single island dissolution rate in a zero effective chemical potential, and for the surface diffusion coefficient are in good agreement with previous studies of step capillary wave motion, and the decay of surface gratings by surface diffusion, capturing this variety of phenomena in a single, coherent framework. This encourages us to expect that molecular beam epitaxy or chemical vapor deposition growth, which—aside from the presence of nucleation—only differs from ripening by having the chemical potential controlled by external, rather than internal sources, can be understood in the same general terms.

N.C.B. was supported by the NSF under Grant No. DMR91-03031. W.T. acknowledges a grant from the German Max-Planck Gesellschaft. We thank Mark Reuter for his assistance with the experiment.

-
- [1] N. C. Bartelt, R. M. Tromp, and E. D. Williams, *Phys. Rev. Lett.* **73**, 1656 (1994).
 - [2] P. W. Voorhees, *Ann. Rev. Mater. Sci.* **22**, 197 (1992); *J. Stat. Phys.* **38**, 231 (1985).
 - [3] M. Marder, *Phys. Rev. A* **36**, 858 (1987).
 - [4] M. G. Lagally, R. Kariotis, B. S. Swartztruber, and Y. W. Mo, *Ultramicroscopy* **31**, 87 (1989).
 - [5] M. Zinke-Allmang, L. C. Feldman, and M. H. Grabow, *Surf. Sci. Rep.* **16**, 377 (1992).
 - [6] O. Krichevsky and J. Stavans, *Phys. Rev. Lett.* **70**, 1473 (1993).
 - [7] W. Telieps and E. Bauer, *Ultramicroscopy* **17**, 57 (1985); R. M. Tromp and M. C. Reuter, *Mater. Res. Soc. Proc.* **237**, 349 (1992).
 - [8] L. M. Lifshitz and V. V. Slyozov, *J. Chem. Solids* **19**, 35 (1961).
 - [9] N. C. Bartelt, W. Theis, and R. M. Tromp (to be published).
 - [10] G. R. Carlow and M. Zinke-Allmang, *Can. J. Phys.* **72**, 812 (1994), and references therein.
 - [11] To compute the Voronoi polygons we used the algorithm of I. K. Crain, *Comput. Geosci.* **4**, 131 (1978).
 - [12] M. E. Keeffe, C. C. Umbach, and J. M. Blakely, *J. Phys. Chem. Solids* **55**, 965 (1994).

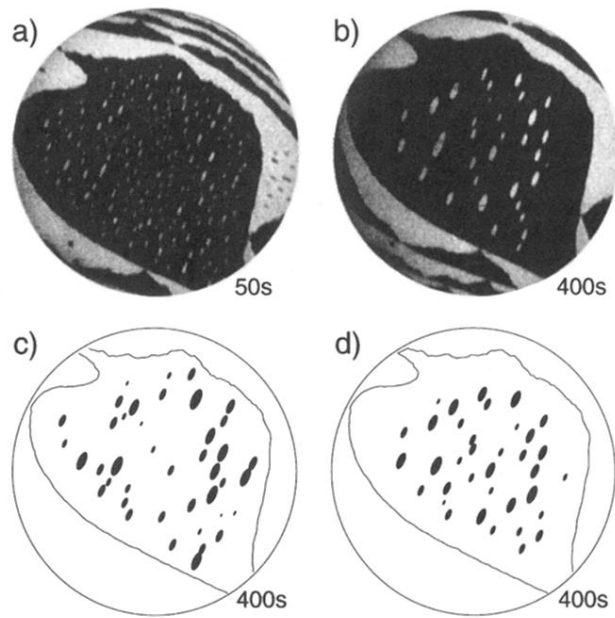
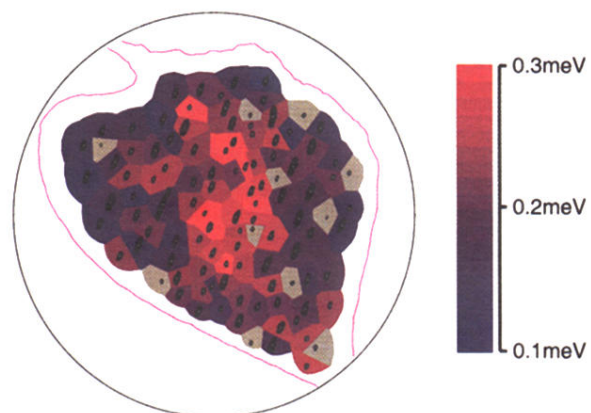


FIG. 1. Experimental and simulated island configurations on Si(001). Panels (a) and (b) show LEEM images at 50 and 400 s after the temperature was raised to 670 °C. Alternate dark and bright regions differ in height by one atomic layer. The field of view is $5.5 \mu\text{m}$. The experimental image at 400 s is contrasted with the island configurations resulting from propagating the experimental configuration at 50 and 400 s using a mean-field [panel (c)] and a nearest-neighbor approach [panel (d)].

a) Experiment at 100s



b) Nearest-neighbor theory

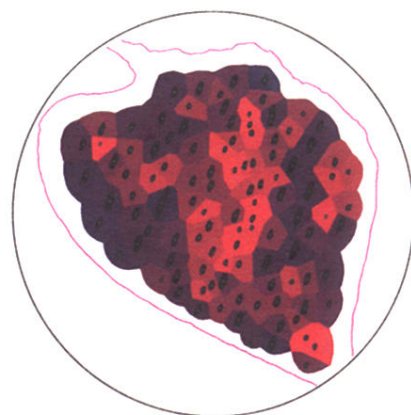


FIG. 3(color). Comparison of the experimentally determined chemical potential map at 100 s [panel (a)] with the results of the nearest-neighbor model [panel (b)]. Gray areas in the experimental plot indicate islands that are too small to derive a reliable chemical potential from. The Voronoi polygon surrounding each island is colored according to the chemical potential obtained from a measurement of the island's growth rate.